Sub-15 nm nanoimprint molds and pattern transfer

Debbie Morecroft, Joel K. W. Yang, S. Schuster, and Karl K. Berggren[a)]
Department of Electrical Engineering and Computer Science, Massachusetts Institute of Technology, Cambridge, Massachusetts 02139

Qiangfei Xia, Wei Wu,[b)] and R. Stanley Williams
Information and Quantum Systems Lab, Hewlett-Packard Laboratories, Palo Alto, California 94304

(Received 16 July 2009; accepted 26 October 2009; published 3 December 2009)

This work addresses the challenges in fabricating sub-10 nm sized features, dense (sub-15 nm half-pitch) arbitrary-pattern nanoimprint molds, as well as pattern transfer of the molds using nanoimprint. The molds were fabricated using an optimized electron-beam lithography process with hydrogen silsesquioxane (HSQ) resist. Two different mold-processing routes were investigated: (1) HSQ patterns on top of a silicon substrate were directly used for nanoimprint and (2) the HSQ patterns on the mold were transferred into the underlying silicon substrate to increase the aspect ratio of the patterns prior to imprint. After the nanoimprint, lift-off was carried out to demonstrate that the pattern could be transferred into functional materials. The difference between the two mold-processing routes is discussed. The results show excellent resolution transfer throughout the process flow to create sub-15 nm half-pitch patterns in functional materials. © *2009 American Vacuum Society.* [DOI: 10.1116/1.3264670]

I. INTRODUCTION

Nanoimprint lithography is capable of high throughput, low cost, and high resolution,[1] but generally relies on other techniques, such as molecular-beam epitaxy followed by selective wet etching,[2,3] or spatial-frequency doubling[4] to fabricate sub-20 nm half-pitch molds. These techniques are typically limited in the flexibility of pattern design, permitting, for example, only simple periodic linear patterns to be formed. In contrast, electron-beam lithography (EBL) is capable of directly writing high-resolution arbitrary patterns, but its throughput is limited due to limited beam current at high resolution and serial nature of the pattern exposure. The challenge of manufacturing new nanodevices requires advancements in nanofabrication techniques, to allow for the fabrication of arbitrary, high-resolution (sub-15 nm half-pitch and sub-10 nm feature size) patterns while at the same time providing high throughput at low cost. In this work we address this challenge by performing nanoimprint lithography using EBL-patterned nanoimprint molds, thereby combining the attributes of EBL and nanoimprint lithography. In addition, we demonstrate pattern transfer of the nanoimprinted nanostructures into functional materials.

To demonstrate sub-10 nm nanoimprint and pattern transfer a number of processing steps have to be developed, all at high resolution. HSQ was chosen as the electron-beam resist because previous work has shown that the contrast can be enhanced by using a salty-development technique.[5] The patterns were written using a Raith 150 EBL tool at 30 kV acceleration voltage. Figure 1 shows some of the complex patterns that were created in the HSQ resist, including hexagonal/square-packed dot arrays, nested-L's and dot/line combinations. Figure 2 is a schematic showing the two different process-flow approaches for fabricating the nanoimprint mold; in the first, the HSQ patterns on the silicon were directly imprinted into the nanoimprint resist, and in the second the patterns were first transferred into the underlying silicon using reactive ion etching (RIE) to increase the aspect ratio of the structures. Typically the electron-beam resist must be thin (20–30 nm) to achieve high pattern resolution, but this also means that the imprint into the nanoimprint resist will be shallow. The nanoimprint resist has two functions; it must faithfully reproduce the features on the mold, and subsequently it must act as a mask for either etching or lift-off. The advantage of using RIE for pattern transfer is that the subsequent imprint in the resist can be deeper and better defined, making the subsequent etch or lift-off step easier. However, feature resolution might be lost during etching due to "waist" formation or tapering of the structures.[6] Previous work has shown that the etch-mask properties of HSQ can be improved by thermal[7] or by electron-bombardment-based curing.[8] However, there are relatively few publications on RIE pattern transfer of sub-15 nm half-pitch patterns, probably due to the difficulty of fabricating such dense structures with EBL due to proximity effects. Lister *et al.* achieved 23 nm pitch period gratings and sub-15 nm dots by using the EBL to pattern diamond substrates, since the low atomic number of carbon reduces the backscatter of the electron beam and improves the image contrast.[9] Other work has reported pattern transfer for 30 (Ref. 10) and 25 nm (Ref. 11) lines and spaces using inductively coupled plasma etching.

II. EXPERIMENT AND RESULTS

The following section describes how the mold was fabricated and characterized, how the nanoimprint was carried out, and finally the results of the pattern transfer into a functional material using lift-off.

[a)]Electronic mail: berggren@mit.edu
[b)]Electronic mail: wei.wu@hp.com

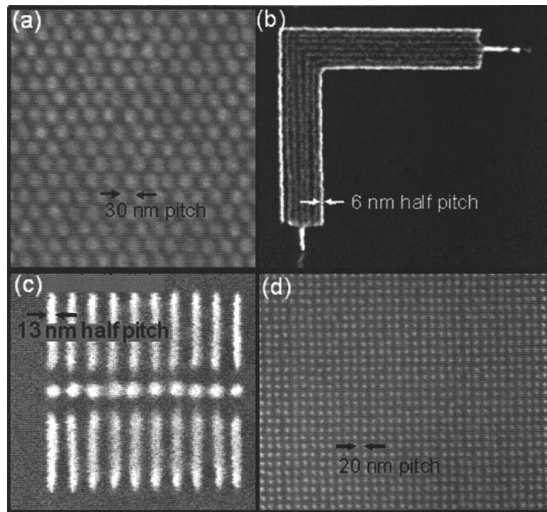

FIG. 1. Scanning electron micrographs showing square packed hexagonal/square dots arrays, nested L's, and dot/line patterns in HSQ resist on a silicon substrate. Images were taken at 10 kV and 30 μm aperture.

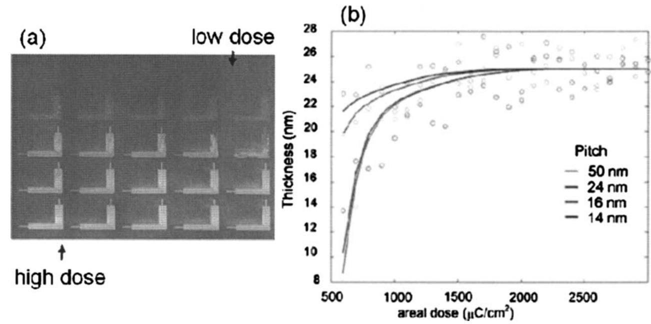

FIG. 3. (a) Scanning electron micrograph showing a typical dose matrix written for the nested L patterns. Imaging was carried out at 10 kV with a 30 μm aperture. (b) Atomic force microscopy (AFM) measured (open circles) and calculated (lines) thickness vs array position.

A. Mold fabrication and characterization

Initially optical lithography and evaporation were used to pattern large (50–500 μm) Cu/Au alignment marks to help find the nanostructures in the proceeding steps. The HSQ resist was purchased from Dow Corning (XR-1541) and spun to a thickness of between 20 and 30 nm on a 4 in. silicon wafer. No postbake was used and the resist was exposed in a Raith 150 SEBL at 30 kV acceleration voltage. The nanostructure patterns were designed to test the resolution limit of the nanoimprint and included nested-"L," hexagonal/square packed dots and dot/line combinations (Fig. 1). Single-pixel lines and dots were written using dose matrices in the exposure layout. Although the elements in the arrays were spaced by ~500 nm and were within the backscatter range of the electrons (~10 μm), the extra dose contributed by backscattering from neighboring elements were still small compared to the exposure dose from the forward scattered electrons. Exposure line doses were between 5.8 and 18.6 nC/cm and the dot areal doses for the square array were between 3000 and 9400 $\mu C/cm^2$. The pitches of the patterns were varied from 12 to 50 nm, to test the resolution limits. The patterns were developed in an aqueous solution of 1 wt % NaOH 4 wt % NaCl, which was previously shown to give a high development contrast.[5] After development the mold was cured to harden the HSQ, either in oxygen plasma or by rapid thermal annealing at 800 °C for 10 min. No significant difference was found between these two annealing methods.

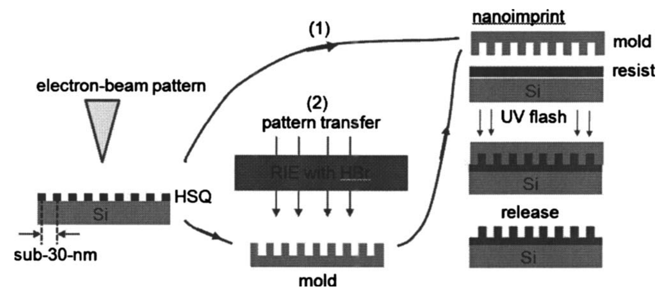

FIG. 2. Schematic showing the two different process flow approaches for making the nanoimprint mold. For process flow (1) the HSQ patterns on the silicon substrate are directly used as the nanoimprint mold. For process flow (2) the patterns are transferred into the silicon substrate using a HBr plasma etch, and then used as the nanoimprint mold.

For both direct imprint and RIE pattern transfer, it was important to consider the height of the features, which depended on both the exposure dose and development conditions. Dose matrices were written and the heights of the features were measured using atomic force microscopy (AFM). Figure 3 (left) is a scanning electron micrograph showing a typical dose matrix for the nested-L patterns. In this image the exposure dose increased from the top right to the bottom left of the matrix. The thickness of resist remaining after development was measured using AFM and plotted as a function of the position in the array (Fig. 3, right) for patterns with increasing pitch from 14 to 50 nm (shown as open circles on the graph). Previous work has shown that the contrast curve of HSQ could be fitted with the following phenomenological function:

$$\mathrm{RTR} = \frac{T}{1+\eta}[(1-e^{-(D-D_0)/A}) + \eta(1-e^{-(D-D_0)/B})],$$

where RTR is the resist thickness remaining after development, T is the original resist thickness, D is the electron areal dose during exposure, D_0 is the areal dose at the onset of incomplete development, and A, B, and η are fitting parameters. The results obtained in our experiments are in agreement with the previous work, in that the calculated contrast curves (solid lines on the graph) are in close agreement with the experimental results. The results show that the height of the nanostructures did not change significantly with dose for the 14 and 16 nm pitch patterns. However, it did change significantly for 24 and 50 nm pitch features below position 5 in the array. These results were used to give an indication of the best dose for each pattern pitch.

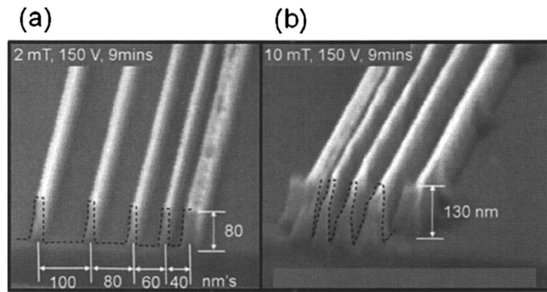

FIG. 4. Cross-sectional scanning electron micrographs of long HSQ lines etched into silicon using RIE with a HBr plasma at (a) 2 mT and (b) 10 mT chamber pressure. The mask erosion by ion bombardment can be seen. Imaging was carried out at 10 kV with a 30 μm aperture.

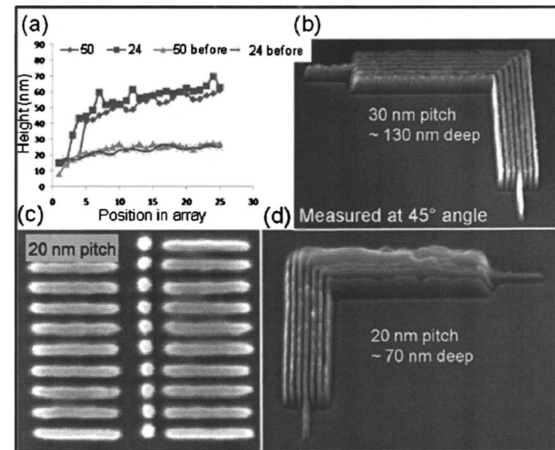

FIG. 5. (a) AFM measurements showing feature height vs position in the array for 50 nm and 24 nm pitch before and after etching. Also shown are scanning electron micrographs of (b) and (d) 45° scanning electron micrographs of 30 nm and 20 nm pitch nested "L's" and (c) a top-down complex pattern with lines and dots. Imaging was carried out at 10 kV with a 30 μm aperture.

B. Etching of the mold with RIE

Reactive-ion etching of the patterns was done in a hydrogen bromide (HBr) plasma, as this plasma chemistry has been shown to give a good etch selectivity between HSQ (silicon oxide) and silicon.[6] Initially, long lines were written with pitches varying between 100 and 20 nm, so that they could be cleaved and the change in cross section with different etch conditions could be studied. Figure 4 shows how the cross section of the lines changed for (4a) 2 mT and (4b) 10 mT chamber pressures, while keeping the same etch duration. A gradual widening of the feature size could be seen with increasing etch depth, which indicated that it was better not to etch deeper than 70 nm for the smaller-pitch samples. For the purpose of the nanoimprint mold, 70 nm deep features were more than sufficient. Also, more mask erosion was evident at 10 mT chamber pressures. The etch rate of Si [measured using scanning electron micrpscopy (SEM)] at 10 mT was ~14 nm/min and at 2 mT it was ~10 nm/min. A series of experiments were carried out varying the pressure, as well as voltage and power of the plasma etch, to optimimize transfer of the fine features. The optimum was 2 mT pressure and a constant voltage of 150 V. These conditions were then applied to the etching of the nanopatterns, as shown in Fig. 5. AFM characterization was also carried out before and after etching 50 nm and 24 nm pitch patterns, as shown in Fig. 5 (top left). The results show that the height of the 50 nm and 24 nm pitch nested-L's before etching was ~20 nm. After etching the height increased to ~60 nm. Since the width of the features was sub-10 nm, this corresponds to an aspect ratio of at least 1:6. Figure 5 also shows angled (45°) and planar scanning electron micrographs of some of the etched patterns. The results show excellent pattern-transfer resolution with sub-15 nm half-pitch. No significant broadening of the feature width can be seen, although the finer 20 nm pitch structures clearly showed more erosion due to the ion bombardment. It might be possible to further reduce this erosion by optimizing the etch conditions and/or reducing the etch depth.

C. Nanoimprint

The UV-cure nanoimprint was carried out at HP Laboratory. The nanoimprint was carried out using a unique wafer bowing technique, which reduces the mechanical distance between the mold and the wafer and enables high-quality nanoimprint.[12] More details of the nanoimprint process can be found in the given reference, but the basic process steps are as follows: (1) the mold is cleaned with an oxygen plasma, (2) a mold releasing layer (trichloro (1*H*,1*H*,2*H*,2*H*-perfluorooctyl)silane) is formed by self-assembled monolayer, (3) a double-layer nanoimprint resist is spin coated onto a wafer including a transfer layer and a liquid imaging layer, (4) the mold and wafer are brought into contact at an imprint pressure of 1 atm, (5) the UV-light cures the resist, and finally (6) the mold and wafer are separated. Figure 6 shows SEM images of the nanopatterns in the imprint resist (coated with a thin metal layer to prevent charging), for direct imprint (top two images) and etch and imprint (bottom two images). The results for the direct imprint show 7 nm holes with 10 nm half-pitch. The 15 nm half-pitch nested-L's show that sharp corners and dense lines were successfully imprinted as resolving individual lines. The results show excellent pattern-transfer resolution between the mold and imprint resist. The etch-and-imprint results also easily resolve 12.5 nm half-pitch complex patterns. It is interesting to note that for the etch-and-imprint results, the isolated features tended to be wider than for the dense features, as indicated in Fig. 6. It is unclear why this should occur, but it may have been due to the resulting deeper imprints, which caused more displacement and hence larger distortion of the imprint resist. The results show that both nanoimprint mold-processing routes were successful, since both nanoimprints showed high-resolution results.

D. Transfer into functional materials

In order to make useful applications, patterns on the nanoimprint resist imaging layer have to be transferred. Finally and perhaps most importantly was the transfer of the

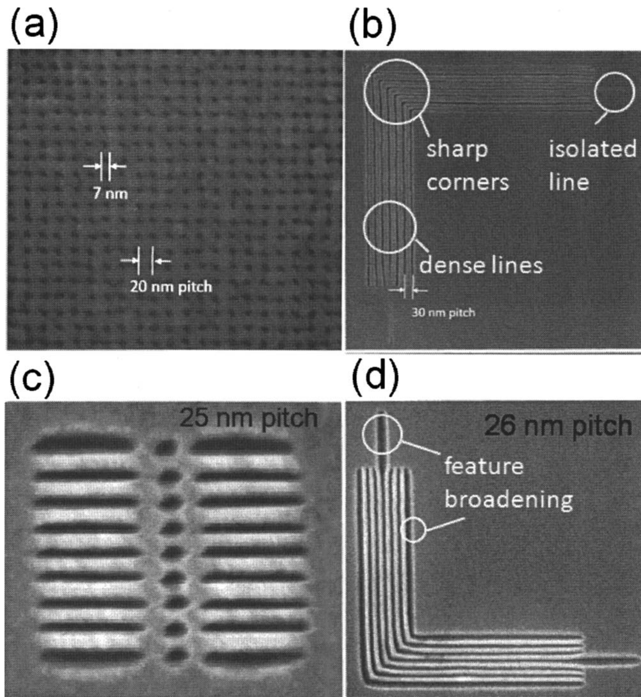

FIG. 6. Scanning electron micrographs for (a) and (b) direct imprint and (c) and (d) etch and imprint. Imaging was carried out at 10 kV with a 30 μm aperture. The direct imprint of the nested L shows sharp corners and high resolution of both the dense and isolated lines.

nanoimprinted pattern into a functional material. After the direct nanoimprint was complete the residue imprint layer was removed and the pattern was transferred into the transfer layer using CF_4 and O_2 based RIE, respectively. To minimize the lateral etching, which is common in O_2 RIE, the transfer layer was etched at -20 °C and at a pressure of 2 mT. Metal deposition was carried out using evaporation to minimize conformality of the deposited film. After the imprint resist was removed by a warm acetone lift-off process, metal nanostructures remained where the HSQ patterns were originally positioned. The entire process is therefore a positive process; producing functional material in the same place as the original HSQ mask. Figure 7 shows some examples of the metal nanostructures produced from the direct imprint mold, including a 12 nm half-pitch nested-L and a 15 nm half-pitch square-packed dot array. Both structures have a 1 nm Ti/5 nm Pt stack.

III. CONCLUSION AND OUTLOOK

The key result of this article is the demonstration that it is possible to combine EBL and nanoimprint to pattern sub-10 nm feature size and sub-15 nm half-pitch arbitrary patterns in functional material. Two different process routes were investigated including direct imprint of electron-beam patterned features and pre-etching of the mold before the imprint. Both process routes were successful, with the direct imprint showing a slightly higher resolution, but at the expense of more shallow imprint features. The imprint results showed that there needs to be a compromise between pattern resolution and imprint depth. Finally, dry etching of the mold was carried out using a HBr plasma, which showed good selectivity between the HSQ patterns and the silicon substrate. The etch results show 10 nm half-pitch features etched to a depth of 70 nm, which to the best of our knowledge is the highest-resolution dense feature reported to date.

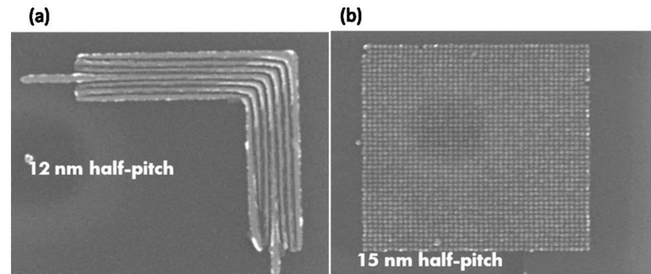

FIG. 7. Pattern transfer of the nanoimprint patterns into metal. (a) 12 nm half-pitch nested L and (b) 15 nm half-pitch square packed dot array.

ACKNOWLEDGMENTS

The authors acknowledge financial support from the Alfaisal University and the King Abdulaziz City for Science and Technology. This work made use of MIT's shared scanning-electron-beam-lithography facility in the Research Laboratory of Electronics (SEBL at RLE). They thank James Daley and Mark Mondol for helpful discussions. The work at HP was sponsored in part by DARPA.

[1]S. Y. Chou, P. R. Krauss, and P. J. Renstrom, Appl. Phys. Lett. **67**, 3114 (1995).
[2]M. D. Austin, W. Zhang, H. Ge, D. Wasserman, S. A. Lyon, and S. Y. Chou, Nanotechnology **16**, 1058 (2005).
[3]G.-Y. Jung *et al.*, Nano Lett. **6**, 351 (2006).
[4]Z. Yu, W. Wu *et al.*, Nanotechnology **17**, 4956 (2006).
[5]J. K. W. Yang and K. K. Berggren, J. Vac. Sci. Technol. B **25**, 2025 (2007).
[6]S. V. Pendharkar *et al.*, J. Vac. Sci. Technol. B **13**, 2588 (1995).
[7]L. O'Faolain, M. V. Kotlyar, N. Tripathi, R. Wilson, and T. F. Krauss, J. Vac. Sci. Technol. B **24**, 336 (2006).
[8]J. K. W. Yang, V. Anant, and K. K. Berggren, J. Vac. Sci. Technol. B **24**, 3157 (2006).
[9]K. A. Lister, B. G. Casey, P. S. Dobson, S. Thorns, D. S. MacIntyre, C. D. W. Wilkinson, and J. M. R. Weaver, Microelectron. Eng. **73–74**, 319 (2004).
[10]A. L. Goodyear, S. MacKensie, D. L. Olynick, and E. H. Anderson, J. Vac. Sci. Technol. B **18**, 3471 (2000).
[11]D. L. Olynick, B. D. Harteneck, E. Veklerov, M. Tendulkar, J. A. Liddle, A. L. David Kilcoyne, and T. Tyliszczak, J. Vac. Sci. Technol. B **22**, 3186 (2004).
[12]W. Wu *et al.*, Nano Lett. **8**, 3865 (2008).